Chinese Journal of Physics 68 (2020) 507–513

Contents lists available at ScienceDirect

Chinese Journal of Physics

journal homepage: www.elsevier.com/locate/cjph

Magnetic field effect on the electronic states and the intraband optical absorption spectrum of a laser dressed double quantum dot molecule

M.G. Barseghyan[a], H.M. Baghramyan[b], L.M. Pérez*[,c], D. Laroze[c]

[a] National University of Architecture and Construction of Armenia, Teryan 105, Yerevan, 0009, Armenia
[b] Istituto Italiano di Tecnologia, Via Eugenio Barsanti, 14, Arnesano LE 73010, Italy
[c] Instituto de Alta Investigación, CEDENNA, Universidad de Tarapacá, Casilla 7D, Arica, Chile

ARTICLE INFO

Keywords:
Magnetic field
Double quantum dot molecule
Optical properties

ABSTRACT

The simultaneous effects of intense terahertz (THz) laser, a homogeneous magnetic fields, and the modification of the structural parameters on the electronic states, and the intraband optical absorption spectrum in a two-dimensional double quantum dot molecule are theoretically investigated. The crossing and anticrossing are observed in the energy dependence on the magnetic field induction between the third and the fourth energy levels. Additionally, it is shown that an intense THz laser field always shifts the energy spectrum to higher values. The variation of the structural parameters leads to the change of the positions of the energy levels and the anticrossing point. Finally, we have found that the intraband optical absorption spectrum, particularly the absorption intensity and the peak position, can be effectively regulated by an intense THz laser and a magnetic fields, as well as by the variation of the structural parameters of the double quantum dot molecule.

1. Introduction

In the last decades, self-assembled quantum dots (QDs) have become of major importance for both, the research of confined electronic states and its applications in the next-generation of optoelectronic devices [1–11]. Nanostructures generated by a coherent tunneling between the “atomic” constituents and formed by two or more QDs are similar to “natural” molecules in delocalized molecular states with distinctive properties [12–16]. On the contrary, natural molecules, the states of quantum dot molecules (QDMs) can be tuned by external fields or during the growth. These features turn QDMs into structures of great interest since the point of view of promising elements for future solid state optoelectronic devices.

Lateral QDMs are formed by two QDs disposed side-by-side on the growth surface. Despite the fact that tunnel coupling in lateral QDMs is usually weaker than in vertical QDMs (dots piled along the growth direction), lateral QDMs are compatible with the device generation that simultaneously exploit the charge occupancy and the interdot coupling by the application of electric fields [17,18].

The effective controlling of molecular states in double QDMs by external magnetic field has already been theoretically demonstrated [19–21]. The total-spin phase diagram of the two-electron QDM as a function of the magnetic field induction and the interdot distance were demonstrated in Harju et al. [19], Helle et al. [20], showing the possibility to use the system for a quantum computer gate. The creation of molecular states in a two-electron QD dependent on the barrier potential was realized in Dybalski and Hawrylak

* Corresponding author.
E-mail address: lperez@uta.cl (L.M. Pérez).

https://doi.org/10.1016/j.cjph.2020.09.028
Received 10 June 2020; Received in revised form 15 September 2020; Accepted 21 September 2020
Available online 01 October 2020
0577-9073/ © 2020 The Physical Society of the Republic of China (Taiwan). Published by Elsevier B.V. All rights reserved.

[21]. Additionally, the analysis of the variations of the singlet-triplet gap as a function of the barrier potential and an external magnetic field was done. On the other hand, the ferrimagnetic and ferromagnetic phases were detected in spin phase diagrams of laterally coupled double QDMs [22]. Therein, the confinement potential is a sum of three Gaussians, and single-electron states in the presence of an external magnetic field have been illustrated. Furthermore, in QDMs was demonstrated as a charge detection system which allows controlling charge states and tunnel coupling [23]. The average occupation in one dot was measured by an integrated electrometer to describe a single electron state in QDM.

The first systematic study of the combined effect of intense THz laser field and strong magnetic field on interacting electrons in so-called artificial atoms (QDs) has been done in Ref. [24]. It was demonstrated that the electromagnetic fields result in a non-perturbative symmetry breaking and related transitions in the ground state of the correlated electronic system “dressed” with photons. These processes are controlled by the polarization and intensity of the radiation. A new way of controlling the molecular states in the system of quantum nanostructures was suggested in Baghramyan et al. [25]. In particular, the molecular states in laterally coupled double quantum rings are effectively controlled by THz laser and electric fields. It was shown that an intense laser field (ILF) is able to dissociate the quantum ring molecule adding 2-fold degeneracy to the molecular states given the overlapping length between the rings.

Recently, we have studied the mechanism of the passage between a double into a single quantum dot produced by THz laser field [26]. It has been shown that the THz laser field creates Fock-Darwin states in a double QDMs with anisotropic confinement potential. In the present work, we suggest an alternative approach of tuning the intraband optical features of double QDM and the molecular states. We demonstrate, that except for the THz ILF and the magnetic field applied perpendicularly to the plane of the double QDM the molecular states can be effectively controlled by varying the structure parameters of the system. This combination of the fields on QDM, to the best of our knowledge, has never been studied. The paper is arranged as follows: In Section 2 the theoretical model is presented. In Section 3 the results and the corresponding discussion are presented. Finally, the conclusions are presented in Section 4.

2. Theoretical model

We study the single electron states in laterally coupled double QDM under the action of a magnetic field and a ILF. The confinement potential of the QDM is modeled as a perturbed two-dimensional parabolic potential by a Gaussian barrier given by the following expression [21,26]:

$$V(x, y) = \frac{1}{2}m\omega^2(x^2 + y^2) + V_0 e^{-\frac{x^2}{R^2}}. \tag{1}$$

Here ω is the oscillator frequency of the confinement potential, R and V_0 are the width and height of the Gaussian barrier, respectively. The Hamiltonian of the system under the influence of electromagnetic fields is:

$$\left[\frac{1}{2m}\left(\hat{\mathbf{p}} - \frac{e}{c}(\mathbf{A}(t) + \mathbf{A}_m)\right)^2 + V(x, y)\right]\Phi(x, y, t) = i\hbar\frac{\partial}{\partial t}\Phi(x, y, t), \tag{2}$$

where m is the electron effective mass, $\hat{\mathbf{p}}$is the lateral momentum, e is the absolute value of the electron charge. The laser field is only time-dependent (dipole polarization is considered) and linearly polarized along the x- axis with $\mathbf{A}(t) = A_0\mathbf{e}_x\cos(\omega t)$vector potential (only time is considered). The vector potential of the homogeneous magnetic field is $\mathbf{A}_m = (0, Bx, 0)$,where B is the magnetic field induction. Since $\mathbf{A}(t)\cdot\mathbf{A}_m = 0$and the laser field is only time-dependent [27] the Kramers-Henneberger unitary transformation can be applied [28]. Furthermore, we are intereseted in the high-frequency limit cases [29–34], for which the Floquet theory allows to obtain the following time-independent Schrödinger equation [35,36]:

$$\left[\frac{1}{2m}\left(\hat{\mathbf{p}} - \frac{e}{c}\mathbf{A}_m\right)^2 + V_d\right]\Phi_d(x, y) = E_d\Phi_d(x, y). \tag{3}$$

Here, $V_d = V_d(x, y, \alpha_0)$and Eq. (3) shows the time-averaged laser-dressed potential, given by [27]

$$V_d(x, y, \alpha_0) = \frac{\omega_0}{2\pi}\int_0^{2\pi/\omega_0} V(x + \alpha_0 sin(\omega_0 t), y)dt\,, \tag{4}$$

where $\alpha_0 = (8\pi e^2 I/m^2\varepsilon_h^{1/2}c\omega_0^4)^{1/2}$is the amplitude of the quiver motion of the electron under the ILF. I stands for the intensity and ω_0 for the frequency of the ILF and $\varepsilon_h$is the high-frequency dielectric constant.

We are also interested in the intraband optical absorption coefficient. The incident light is x-axis polarized, so the absorption coefficient is given by the following expression [37–39]:

$$\alpha(\omega) = A\frac{\hbar\omega\Gamma|M_{fi}|^2}{(\hbar\omega - \Delta E)^2 + \Gamma^2}, \tag{5}$$

where $\Gamma = 0.2$ meV is the broadening parameter [40,41], $A$is the material constant [42–44], $M_{fi} = \langle f|x|i\rangle$is the intraband matrix element [45], with $|i\rangle$ and $\langle f|$ denoting the initial (ground) and final states, accordingly.

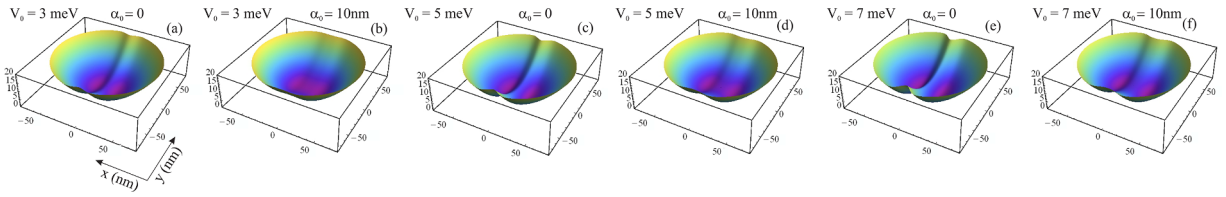


Fig. 1. Confinement potential for double QDM. The results in the frames (a), (c) and (e) are for $\alpha_0 = 0$,and in (b), (d) and (f) are for $\alpha_0 = 10$ nm. The rest of the parameters are $B = 0$,$\hbar\omega = 3$ meV and $R = 10$ nm.

3. Numerical results and discussion

We consider a GaAs double QDM with $m = 0.067m_0$effective mass, where m_0 is the free electron mass, and $\varepsilon_h = 10.5$[46]. The eigensystem (3) is solved using the finite element method in COMSOL Multiphysics [47]. The simulation domain is a square with $40R$ side, such that R characterizes the interdot distance.

3.1. Electronic states

First, we study the influence of the ILF and the double QDM parameters on the dependence of the energy levels on the magnetic field. Fig. 1 demonstrates that the Gaussian barrier height V_0 decreases under the action of ILF. For instance, the $V_0 = 3$ meV height is almost eliminated by the laser field. These effects are reflected in the distribution of the ground state probability density shown in Fig. 2. In the case of an undressed potential the increment of the barrier height separates the probability density into two parts since the coupling of the states in the dots is diminished. On the other hand, the ILF impact strengthens the coupling, and the mentioned separation can be obtained for bigger values of V_0.

The energy as a function of the magnetic field is presented in Fig. 3 considering different values of V_0 and $\alpha_0$and fixed $\hbar\omega = 3$ meV and $R = 10$ nm. The energy of the ground state increases monotonically with Bdue to the strengthening of the electron localization. However, for the excited states, the scenario is different and we observe a non-monotonic behavior. Another important point to consider is that an increase of V_0 results in the increment of the energy since the electron localization region is reduced. Additionally, the laser field shifts the energy spectrum to higher values due to the strengthened size quantization by the ILF. Furthermore, we can observe an anticrossing at $B \approx 1.1$T between the third and the fourth energy levels. With the increase of the barrier height, the anticrossing between those energy levels occurs for small values of B.

Let us now focus on the Gaussian barrier width R effect on the electronic states. Fig. 4 demonstrates the undressed and the dressed confinement potential profile for several values of R. For the $R = 0$case, the double QDM profile turns into a single QD, both in presence and absence of the laser field. For bigger values of R the influence of the ILF on the confinement potential is more visible since the interdot distance increases. Also, it can be seen in Fig. 5 that if $R = 0$,the probability density behavior is that of a single QD. With the increment of the interdot distance the probability in the barrier region becomes lower. On the other hand, the augmentation of α_0 can increase the probability in the center of the structure due to the lowering of the barrier height. From the energy spectra shown in Fig. 6 we observe that in the case of $R = 0$,the Fock-Darwin states [3] appear, because the QDM reshapes into a single QD

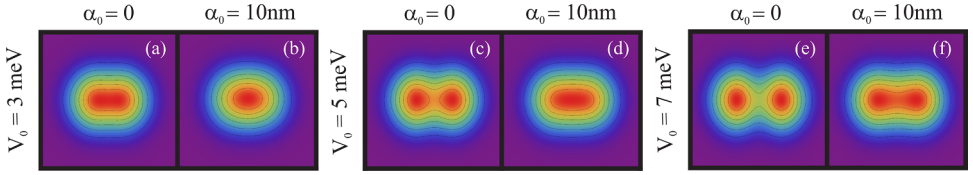


Fig. 2. The probability density plots of the ground state. The results in the frames (a), (c) and (e) are for $\alpha_0 = 0$,in frames (b), (d) and (f) are for $\alpha_0 = 10$ nm. The rest of the parameters are $B = 0$,$\hbar\omega = 3$ meV and $R = 10$ nm.

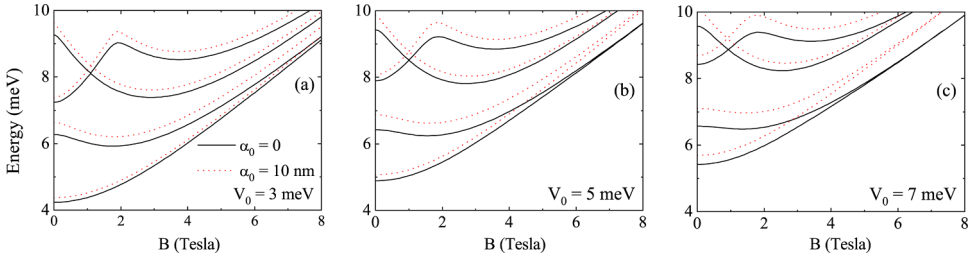


Fig. 3. Low-lying energy levels as a function of the magnetic field induction B for several values of V_0 and α_0. Results are shown for $\hbar\omega = 3$ meV and $R = 10$ nm.

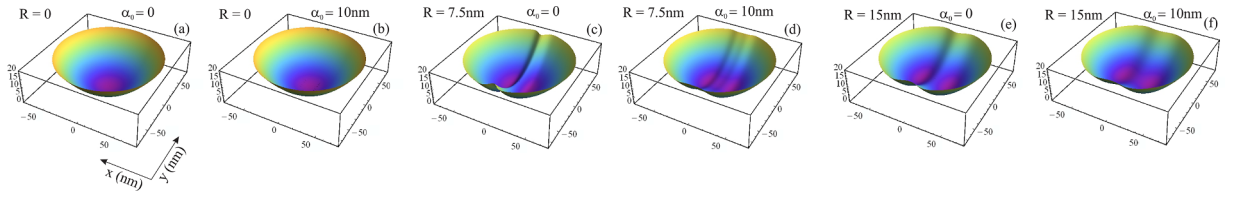


Fig. 4. Confinement potential for a double QDM. Several values of the ILF parameter α_0 and the Gaussian barrier width R have been investigated. The results in the frames (a), (c) and (e) are for $\alpha_0 = 0$,and in frames (b), (d) and (f) are for $\alpha_0 = 10$ nm. The rest of the parameters are $B = 0$, $\hbar\omega = 3$ meV and $V_0 = 5$ meV.

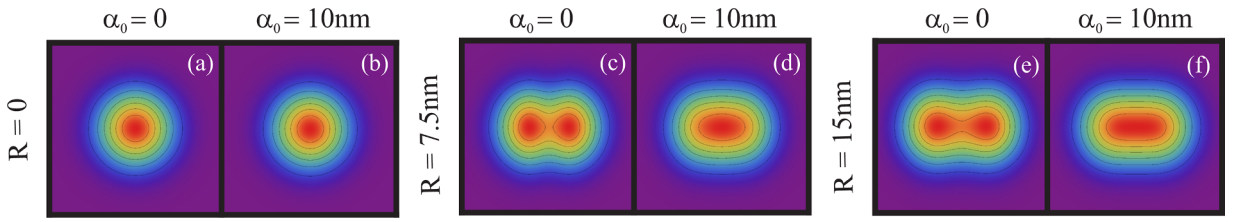


Fig. 5. The probability density plots of the ground state. The results in frames (a), (c) and (e) are for $\alpha_0 = 0$,and in frames (b), (d) and (f) are for $\alpha_0 = 10$ nm. The rest of the parameters are $B = 0$,$\hbar\omega = 3$ meV and $V_0 = 5$ meV.

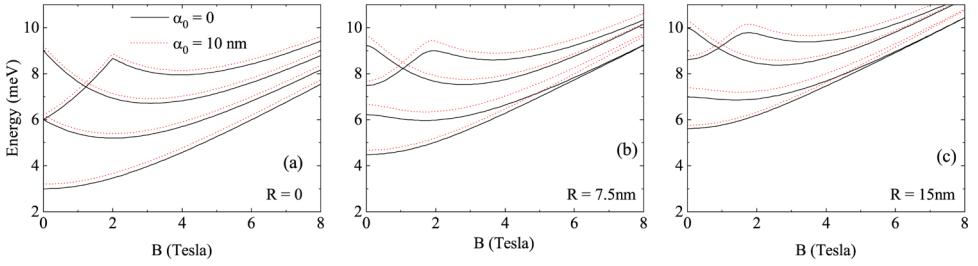


Fig. 6. Low-lying energy levels as a function of the magnetic field induction B, with $\hbar\omega = 3$ meV and $V_0 = 5$ meV.

with 2D isotropic parabolic confinement. For nonzero values of R the structure reshape into double QDM and the degeneracy of the first excited states at $B = 0$disappear. Besides, the increase of R results in higher ground state energies, and the bigger R is, the weaker the magnetic fields will be required to create a crossing of the energy levels of the third and fourth states.

On the other hand, the variation of oscillator frequency ω corresponds to the change of the QD radius. As it is shown in Fig. 7, the bigger ω is, the stronger influence of the ILF on the confinement potential. Moreover, Fig. 8 demonstrates that an increment of α_0 does not significantly change the ground state probability density. However, an increase of $\hbar\omega$ pushes back the electron cloud to the central part of the structure. The energy calculations in Fig. 9 show that for $B = 0$the increment of $\hbar\omega$ shifts the energies to higher values caused by the strengthening of the size quantization. Furthermore, the bigger $\hbar\omega$ is, the less sensitive are the energies to the magnetic field, i.e., the size quantization is stronger than the magnetic one. On the other contrary, the increment of $\hbar\omega$ brings a stronger effect of the ILF. In addition, the energy crossing occurs at higher magnetic field at $\hbar\omega = 5$ meV.

Finally, the results in Fig. 10 demonstrate that the energies are increasing functions of α_0, which means that the confinement

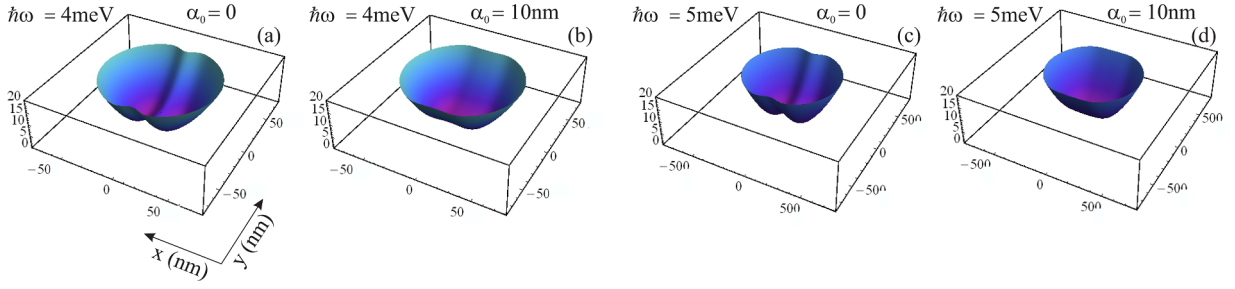


Fig. 7. The confinement potential for a double QDM. Several values of the ILF parameter α_0 and the energy of confinement potential $\hbar\omega$ have been investigated. The results in the frames (a), (c) and (e) are for $\alpha_0 = 0$,and in frames (b), (d) and (f) are for $\alpha_0 = 10$ nm. The rest of the parameters are $B = 0$,$V_0 = 5$ meV and $R = 10$ nm.

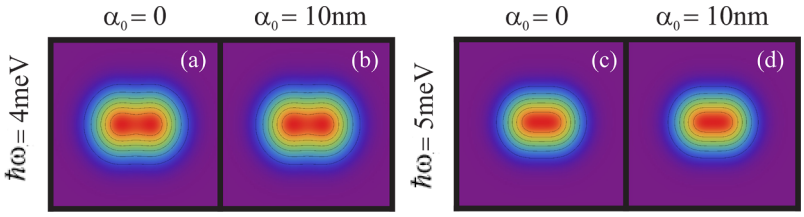


Fig. 8. The plots for ground state probability density. Several values of the ILF parameter α_0 and the energy of confinement potential $\hbar\omega$ are investigated. The results in the frames (a), (c) and (e) are for $\alpha_0 = 0$,in frames (b), (d) and (f) are for $\alpha_0 = 10$ nm. The rest of the parameters are $B = 0$,$V_0 = 5$ meV and $R = 10$ nm.

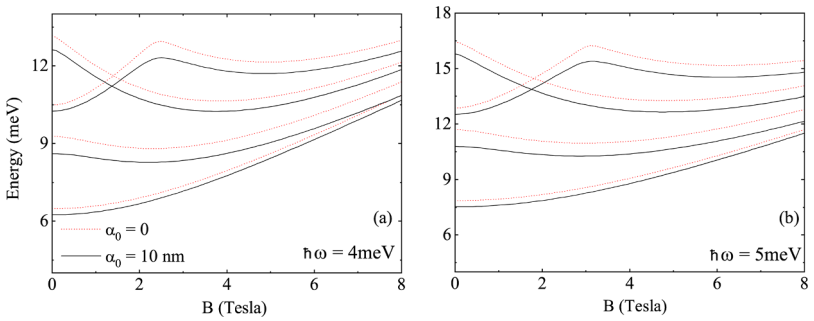


Fig. 9. Low-lying energy levels as a function of the magnetic field induction B for different values of the energy of confinement potential $\hbar\omega$ and ILF parameter α_0. Results are for $V_0 = 5$ meV and $R = 10$ nm.

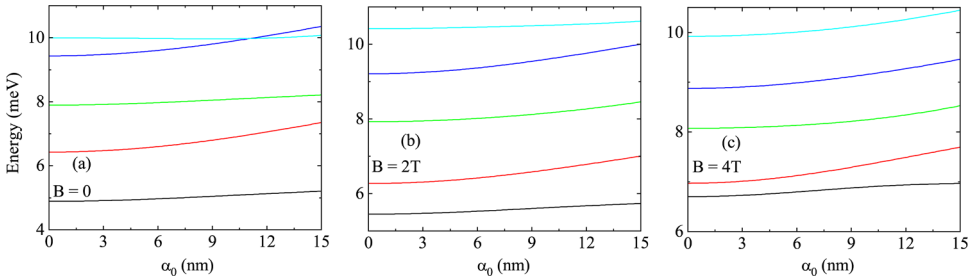


Fig. 10. Low-lying energy levels as a function of $\alpha_0$for different values of B. The results are for $V_0 = 5$ meV, $\hbar\omega = 3$ meV and $R = 10$nm.

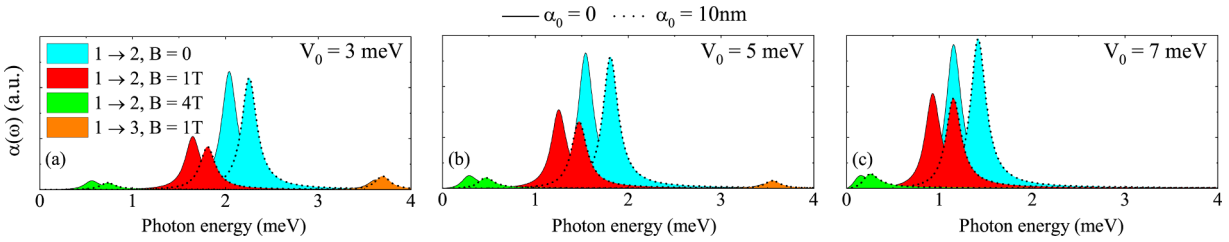


Fig. 11. Intraband absorption coefficient as a function of the incident photon energy for different values of B, $\alpha_0$and V_0. The results are for $\hbar\omega = 3$ meV and $R = 10$ nm.

potential becomes more contracted. It is also interesting to see the disappearance of energy crossing between the fourth and the fifth levels once the magnetic field takes non-zero values.

3.2. Intraband absorption

This subsection is devoted to the analysis of the intraband absorption in double QDM. Fig. 11 demonstrates that the increment of B and V_0 results in the redshift of the absorption spectrum in the absence and presence of ILF. The studies of $1 \rightarrow 3$ transition show that for higher values of V_0 its probability gets lower: for $V_0 = 7$ meV case $1 \rightarrow 3$ the absorption peak value is very small compared to other cases and is not shown in the Fig. 11(c). Also, it can be seen that, due to the large value of the overlap integral of the ground and

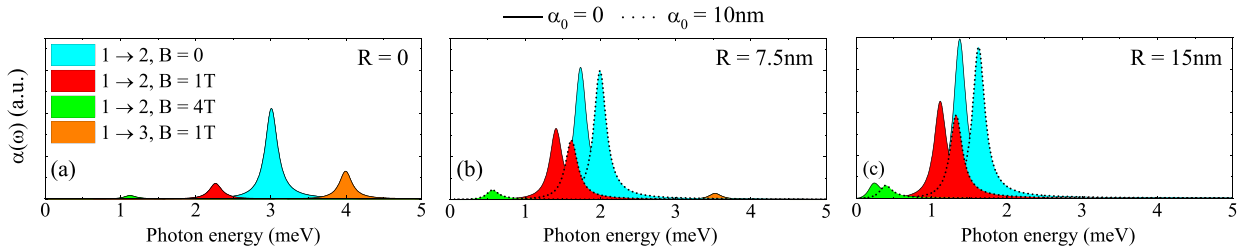


Fig. 12. Intraband absorption coefficient as a function of the incident photon energy for different values of B, $\alpha_0$and R. The results are for $\hbar\omega = 3$ meV and $V_0 = 5$ meV.

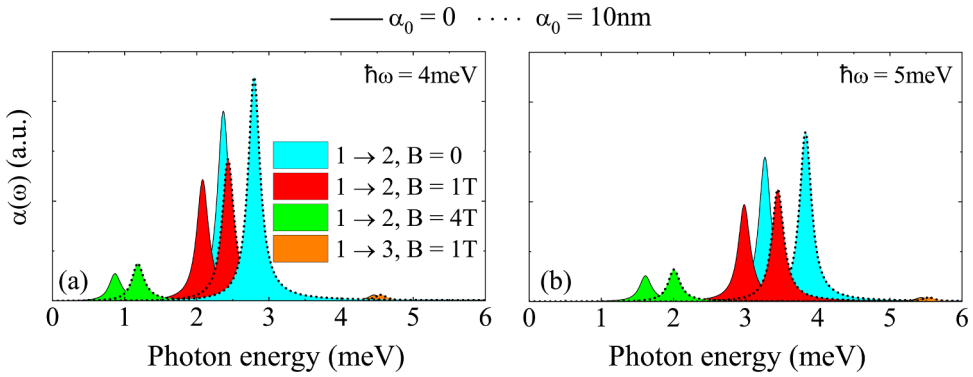


Fig. 13. Intraband absorption coefficient as a function of the incident photon energy for different values of B, $\alpha_0$and $\hbar\omega$. The results are for $R = 10$ nm and $V_0 = 5$ meV.

excited states in the absence of the magnetic field, the absorption coefficient is considerably bigger than in the presence of the magnetic field. From Fig. 12we see that increasing the R value we get a redshift. An interesting fact is that in the cases that $R = 0$, $\alpha_0 = 0$and $\alpha_0 = 10$ nm, the absorption coefficients almost overlap. The latter effect can be understood from Fig. 6(c) where the $\alpha_0 = 0$and $\alpha_0 = 10$ nm are almost equidistant. In addition, as in the case of V_0, the increment of Rresults in the lowering of $1 \rightarrow 3$ transition peak value, which can be expected since the increment of both parameters brings the decreased coupling between QDs. Finally, increasing $\hbar\omega$ results in the blueshift and the lowering of the absorption peak values, as shown in Fig. 13.

4. Final remarks

In conclusion, we have considered the simultaneous effects of intense THz laser, a homogeneous magnetic fields, and the variation of the structural parameters on the electronic states, and the intraband optical absorption spectrum in a two dimensional double QDM. We demonstrated that the ILF can considerably strengthen the coupling between the QDs by lowering the barrier height V_0, which decreases under the action of the ILF. The ground state energy is found to monotonically increase with B, while for excited states a non-monotonic behavior is also possible. An anticrossing is obtained as well between the third and the fourth energy levels occurring for higher magnetic fields if the barrier height is increased. Furthermore, the higher is R, the weaker magnetic field is required to create a crossing. In addition, the increment of the oscillator energy makes energies be less sensitive to the magnetic field but more sensitive to the laser field. The results of the optical response demonstrate that an increment of B, R and V_0 brings the absorption spectrum redshift, while the enlarging of the oscillator energy creates a blueshift.

Declaration of Competing Interest

All the authors declare that they do not have any conflicts of interests.

Acknowledgments

MGB acknowledge the financial support by the Armenian State Committee of Science (Project no. 18T-1C223). LMP and DL acknowledge partial financial support from FONDECYT 1180905. DL acknowledges partial financial support from Centers of excellence with BASAL/ANID financing, AFB180001, CEDENNA.

References

[1] A.J. Shields, Semiconductor quantum light sources, Nat. Photon 1 (2007) 215.
[2] R.J. Warburton, Single spins in self-assembled quantum dots, Nat. Mater. 12 (2013) 483.
[3] S.M. Reimann, M. Manninen, Electronic structure of quantum dots, Rev. Mod. Phys. 74 (2002) 1283.
[4] S.N. Klimin, V.M. Fomin, J.T. Devreese, D. Bimberg, Model of Raman scattering in self-assembled InAs/GaAs quantum dots, Phys. Rev. B 77 (2008) 045307.
[5] V.N. Gladilin, S.N. Klimin, V.M. Fomin, J.T. Devreese, Optical properties of polaronic excitons in stacked quantum dots, Phys. Rev. B 69 (2004) 155325.
[6] R. Khordad, B. Vaseghi, Effects temperature, pressure and spin orbit interaction simultaneously on third harmonic generation of wedge-shaped quantum dots, Chin. J. Phys. 59 (2019) 473.
[7] B. Çakr, U. Atav, Y. Yakar, A. Özmen, Calculation of Zeeman splitting and Zeeman transition energies of spherical quantum dot in uniform magnetic field, Chem. Phys. 475 (2016) 61.
[8] B. Çakr, Y. Yakar, A. Özmen, Investigation of magnetic field effects on binding energies in spherical quantum dot with finite confinement potential chem, Phys. Lett. 684 (2017) 250.
[9] Y. Yakar, B. Çakr, A. Özmen, Magnetic field effects on oscillator strength, dipole polarizability and refractive index changes in spherical quantum dot, Chem. Phys. Lett 708 (2018) 138.
[10] M. Kria, K. Feddi, N. Aghoutane, M. El-Yadri, L.M. Pérez, D. Laroze, F. Dujardin, E. Feddi, Thermodynamic properties of SnO_2/GaAs core/shell nanofiber, Phys. A 560 (2020) 125104, https://doi.org/10.1016/j.physa.2020.125104.
[11] M. Kria, M. El-Yadri, N. Aghoutane, L.M. Pérez, D. Laroze, E. Feddi, Forecasting and analysis of nonlinear optical responses by tuning the thickness of a doped hollow cylindrical quantum dot, Chin. J. Phys. 66 (2020) 444, https://doi.org/10.1016/j.cjph.2020.05.016.
[12] H.J. Krenner, Direct observation of controlled coupling in an individual quantum dot molecule, Phys. Rev. Lett. 94 (2005) 057402.
[13] M.F. Doty, Electrically tunable *g* factors in quantum dot molecular spin states, Phys. Rev. Lett. 97 (2006) 197202.
[14] M.F. Doty, Antibonding ground states in InAs quantum-dot molecules, Phys. Rev. Lett. 102 (2009) 047401.
[15] L. Wang, A. Rastelli, S. Kiravittaya, M. Benyoucef, O.G. Schmidt, Self-assembled quantum dot molecules, Adv. Mater. 21 (2009) 2601.
[16] X. Zhou, Spectroscopic signatures of many-body interactions and delocalized states in self-assembled lateral quantum dot molecules, Phys. Rev. B 84 (2011) 205411.
[17] G. Beirne, C. Hermannstädter, L. Wang, A. Rastelli, O. Schmidt, P. Michler, Quantum light emission of two lateral tunnel-coupled (In, Ga)As/GaAs quantum dots controlled by a tunable static electric field, Phys. Rev. Lett. 96 (2006) 137401.
[18] X. Zhou, M. Doty, Design of 4-electrode optical device for application of vector electric fields to self-assembled quantum dot complexes, J. Appl. Phys. 116 (2014) 163101.
[19] A. Harju, S. Siljamäki, R.M. Nieminen, Two-electron quantum dot molecule: composite particles and the spin phase diagram, Phys. Rev. Lett. 88 (2002) 226804.
[20] M. Helle, A. Harju, R.M. Nieminen, Two-electron lateral quantum-dot molecules in a magnetic field, Phys. Rev. B 72 (2005) 205329.
[21] W. Dybalski, P. Hawrylak, Two electrons in a strongly coupled double quantum dot: from an artificial helium atom to a hydrogen molecule, Phys. Rev. B 72 (2005) 205432.
[22] R.M. Abolfath, P. Hawrylak, Quantum hall ferrimagnetism in lateral quantum dot molecules, Phys. Rev. Lett. 97 (2006) 186802.
[23] M. Pioro-Ladrière, M.R. Abolfath, P. Zawadzki, J. Lapointe, S.A. Studenikin, A.S. Sachrajda, P. Hawrylak, Charge sensing of an artificial H_2^+molecule in lateral quantum dots, Phys. Rev. B 72 (2005) 125307.
[24] P. Hawrylak, P.A. Schulz, J.J. Palacios, Electronic structure of artificial atoms in intense AC terahertz and strong magnetic fields, Solid State Commun. 93 (1995) 909.
[25] H.M. Baghramyan, M.G. Barseghyan, D. Laroze, Molecular spectrum of laterally coupled quantum rings under intense terahertz radiation, Sci. Rep. 7 (2017) 10485.
[26] M.G. Barseghyan, H.M. Baghramyan, A.A. Kirakosyan, D. Laroze, The transition from double to single quantum dot induced by THz laser field, Phys. E 116 (2020) 113758.
[27] M. Gavrila, Atoms in Intense Laser Fields, Academic, New York, 1992.
[28] W.C. Henneberger, Perturbation method for atoms in intense light beams, Phys. Rev. Lett. 21 (1968) 838.
[29] M. Gavrila, J.Z. Kaminski, Free-free transitions in intense high-frequency laser fields, Phys. Rev. Lett. 52 (1984) 613.
[30] M. Pont, N.R. Walet, M. Gavrila, C.W. McCurdy, Dichotomy of the hydrogen atom in superintense, high-frequency laser fields, Phys. Rev. Lett. 61 (1988) 939.
[31] E.C. Valadares, Resonant tunneling in double-barrier heterostructures tunable by long-wavelength radiation, Phys. Rev. B (R) 41 (1990) 1282.
[32] M. Gavrila, Atomic stabilization in superintense laser fields, J. Phys. B 35 (2002) 147.
[33] S. Ganichev, W. Prettl, Intense Terahertz Excitation of Semiconductors, Oxford University Press, 2006.
[34] M. Bukov, L. D'Alessio, Universal high-frequency behavior of periodically driven systems: from dynamical stabilization to Floquet engineering, A. Polkovnikov, Adv. Phys. 64 (2015) 139.
[35] T. Chakraborty, A. Manaselyan, M. Barseghyan, D. Laroze, Controllable continuous evolution of electronic states in a single quantum ring, Phys. Rev. B 97 (2018) 041304. (R)
[36] M.G. Barseghyan, V.N. Mughnetsyan, L.M. Pérez, A.A. Kirakosyan, D. Laroze, Effect of the impurity on the Aharonov-Bohm oscillations and the intraband absorption in $GaAs/Ga_{1-x}Al_xAs$quantum ring under intense THz laser field, Phys. E 111 (2019) 91.
[37] P. Harrison, A. Valavanis, Quantum Wells, Wires and Dots: Theoretical and Computational Physics of Semiconductor Nanostructures, fourth ed., Wiley, 2016.
[38] E. Sadeghi, L.M. M. Moradi, J. Phys, Optical properties of a two-electron system in a double ellipsoidal quantum dot, Chin 54 (2016) 773.
[39] R. Khordad, H. Bahramiyan, S.A. Mohammadi, Influence of impurity on binding energy and optical properties of lens shaped quantum dots: finite element method and arnoldi algorithm, Chin. J. Phys. 54 (2016) 20.
[40] M. Sugawara, Theoretical Bases of the Optical Properties of Semiconductor Quantum Nano-Structures, Semiconductors and Semimetals, 60 Elsevier, New York, 1999.
[41] L. Jacak, P. Hawrylak, A. Wójs, Quantum Dots, Springer, Berlin, 1998.
[42] A. Radu, A.A. Kirakosyan, D. Laroze, H.M. Baghramyan, M.G. Barseghyan, Electronic and intraband optical properties of single quantum rings under intense laser field radiation, J. Appl. Phys. 116 (2014) 093101.
[43] A.K. Manaselyan, M.G. Barseghyan, A.A. Kirakosyan, D. Laroze, C.A. Duque, Effects of applied lateral electric field and hydrostatic pressure on the intraband optical transitions in a $GaAs/Ga_{1-x}Al_xAs$quantum ring, Phys. E 60 (2014) 95.
[44] A. Radu, A.A. Kirakosyan, D. Laroze, M.G. Barseghyan, The effects of the intense laser and homogeneous electric fields on the electronic and intraband optical properties of a $GaAs/Ga_{0.7}Al_{0.3}As$ quantum ring, Semicond. Sci. Technol. 30 (2015) 045006.
[45] H.M. Baghramyan, M.G. Barseghyan, A.A. Kirakosyan, J.H. Ojeda, J. Bragard, D. Laroze, Modeling of anisotropic properties of double quantum rings by the terahertz laser field, Sci. Rep. 8 (2018) 6145.
[46] S. Adachi, Handbook on Physical Properties of Semiconductors, Volume 2: III-V Compound Semiconductors, Springer, Boston, MA, 2004.
[47] COMSOL, Multiphysics, v. 5.3b, COMSOL AB, Stockholm, Sweden.